2024 IEEE/RSJ International Conference on Intelligent Robots and Systems (IROS)
October 14-18, 2024. Abu Dhabi, UAE

A velocity dependent delayed output feedback control (v-DOFC) for gait assistance with an ergonomically designed bi-directional cable-driven hip assist device

Dong Hyun Kim, Junghoon Park, Gyowook Shin, Chiyul Yoon, Yongtae Giovanni Kim, Sang-Hun Kim, Seungyong Hyung, Sungchul Kang, and Minhyung Lee*

Abstract— **Hip assistance with cable-driven devices has been proven to help decrease the metabolic cost of gait. However, most existing devices use heavy actuating modules or provide assistance in only one direction, limiting the effectiveness. Cable-driven devices are also difficult to accurately estimate the hip position using only motor encoders, therefore utilizing various auxiliary sensors. This paper introduces a 1.5 kg cable-driven soft wearable hip assist device that can provide assistance in both flexion and extension, using a velocity-dependent delayed output feedback controller (v-DOFC). The device is designed with the consideration of ergonomics and pressure distribution of wearable parts, to increase the anchoring performance and comfort. The controller uses time-delayed feedback proportional to the velocity output state, allowing control without requiring accurate position estimation. Additionally, directional weighting is used to provide different assistance forces for extension and flexion to match different optimal assistance values. Experimental results show that the device can reduce metabolic cost by 13.8 % compared to walking without the device. The soft wearable hip assist device can be applied to help the elderly with weaker muscles to walk longer distances.**

I. Introduction

Hip assist with wearable devices has been proven to reduce the energy consumption required for walking through various studies. These devices can be categorized into two types: exoskeletons [1-5] and soft cable-driven wearables [6-9]. Various exoskeletons have been developed to assist both flexion and extension, showing a significant reduction in metabolic cost, but they are relatively heavy and rigid frames restrict users' movement.

On the other hand, most of the soft cable driven devices assist one direction (flexion or extension) [6-8]. Unidirectional assistance is proved to help reduce metabolic cost of walking and/or running with larger reduction when extension is assisted [7, 9]. Recently, a cable-driven wearable device that supports both directions of hip has been developed, and it has been shown that more metabolic cost can be reduced when both directions are used [9]. However, the 4 kg weight itself of the device could impact both the metabolic cost and even gait patterns.

In soft cable-driven wearable devices, stable anchoring is crucial to maximize the assistance force delivered by the cable [10]. Previous devices implemented curved waist and thigh straps to increase the contact area and friction [6-8]. However, the shape of the waist with concave and convex curves was not considered (Fig. 1), and the stiff, minimally deformable skeletal structures near the skin (Fig. 1) were not used as anchoring points yet. The anchoring performance could be improved by considering these physical characteristics based on the anatomy of human body.

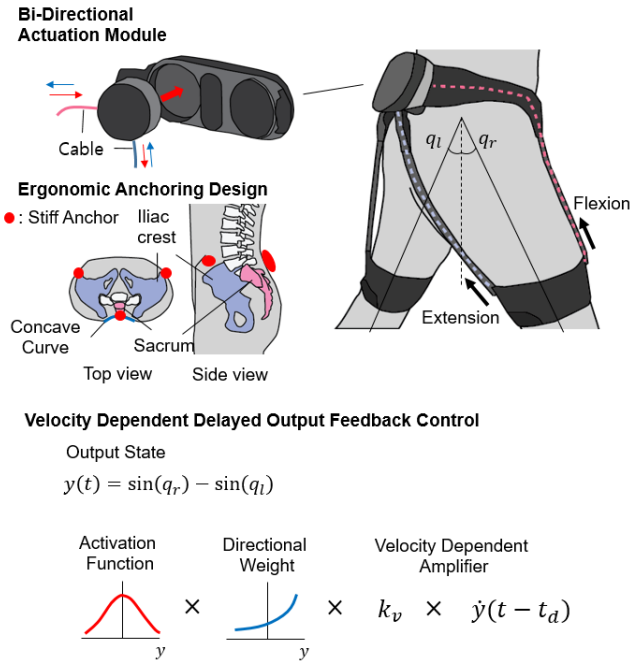

Fig. 1. Overview of the design concept of the proposed device: Bi-directional cable-driven hip assist device with anchoring design considering skeletal anatomy and velocity dependent delayed output feedback control.

Regarding cable-driven devices, most control methods are adopted to estimate the gait phase and various sensors including force, IMU, and foot contact sensors enable precise cable force control [6-9]. In contrast, exoskeletons employ simple control methods with minimal sensors, using motor encoder measurements [3] only, as the hip angle estimation is relatively accurate compared to cable-driven devices.

In this research, we introduce a light weight, bi-directional soft cable-driven wearable hip assist device, along with velocity-dependent delayed output feedback control. The main contributions of this study are 1) the design of a lightweight wearable device applying an ergonomic anchoring design, and 2) proposing a control method for a bi-directional cable-driven device using only encoder values. The controller also includes varied assistance levels depending on the assistance direction.

D. H. Kim, J. Park, G. Shin, C. Yoon, Y. G. Kim, S. Kim, S. Kang, S. Hyung, and M. Lee are with Samsung Research, Samsung Electronics, Seocho-gu, Seoul 06765, South Korea. (*corresponding author to provide phone: +82-2-10-7163-1045; fax: +82-2-6147-7980; e-mail: mhyung.lee@samsung.com).

Fig. 2. Overview of the mechanical design

II. Design of a Soft Wearable Hip Assist Device

A. Overview

The soft wearable hip assist device consists of bi-directional actuation modules, a rear frame, a waist belt, and thigh straps (Fig. 2). The cable-driven actuation modules are mounted on the rear frame. The cable is routed from the actuator through Teflon tubes inside the waist belt, and passes a tunnel composed of elastic straps (flexible bands) placed around the front and rear aspect of the thigh. The cable is then connected with the thigh strap. The cable-driven actuator transmits the force to the cable and assists hip flexion and extension, respectively. When a bidirectional actuator is applied to the proposed device, the total weight is 1.5 kg, and the weight of one actuation module is 240 g. The weight for each component is as in Table 1.

Table I. Weight of Components

Actuation module	240 g (each side)
Thigh strap	87 g (each side)
Rear frame	265 g
Waist belt	284 g
Electronics	87 g
Battery	210 g
Total	1.5 kg

Each component is designed to minimize its weight, since additional weight increases the metabolic cost of walking. The rear frame, waist belt, and thigh straps are designed based on the human skeletal anatomy to provide stable and secure anchoring while reducing pain by distributing pressure. The detailed features of each component are explained in the following sub-section.

B. Bi-directional Cable-driven Actuator

The bi-directional actuation module consists of a cable-driven actuator, a custom motor driver, and a case (Fig. 3(a)). The actuator is powered and communicates via a UART data connection through pogo pins to the main MCU and battery of the rear frame.

The cable-driven actuator was designed to generate assistance force during walking. Such assistance force of the bi-directional actuator was targeted to cover 15 % of the hip torque (15 Nm) required to walk in the speed at 6 km/h for men weighing 70 kg. The target assistance force and linear speed of the cable-driven actuator were set 150 N and 400 mm/s, respectively for a moment arm of 100 mm.

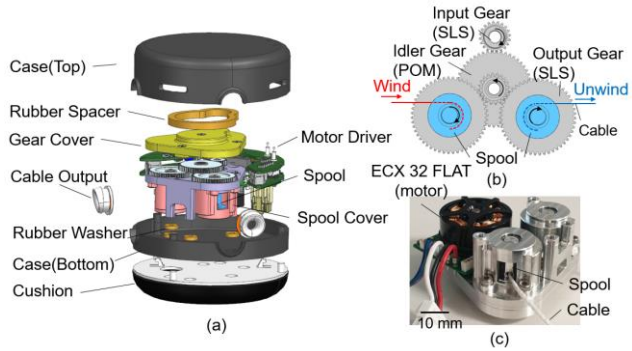

Fig. 3. Bi-directional actuation module: (a) Exploded view, (b) Gear train, (c) Cable-driven actuator

The ECX FLAT 32L 100 W motor (Maxon Group, Sacheln, Switzerland) is used because it is a light, flat, and high torque density motor. Also, it can meet our desired torque and speed requirements. It is done by a reduction ratio of 6.5:1 with a custom designed two-stage gear box consisting of a motor (input) gear, idler gear, and spool (output) gears (Fig. 3(b)). The cable (SK75, 1.5mm thickness, Jeely Sport Products Co., Ltd., Jiangsu, China) was wound around the spool connected to the output shaft (coupled with spool gear). The radius of the spool was set to 4 mm to achieve a force of 147 N and a speed of 627 mm/s. Note that the velocity was set greater than target velocity, since cable-driven systems should have greater speed to compensate slack. Two spools connected with the spool gear driven by the idler gear rotate in opposite directions, so that when one side winds up the cable, the other side unwinds it.

Small spool design could easily encounter derailment of the cable from the spool when unwinding the cable by multiple turns without pretension. We are able to use smaller spools and motors by preventing cable derailment with a cover placed on the spool (Fig. 3(a)). The gap between the cover and the spool's wing along the radial direction (0.25 mm) is designed to be smaller than the thickness of the cable (1.5 mm). Also, the height of the cover hole (Fig. 3(a), pink) is designed to be slightly smaller (0.6 mm smaller) than the winding region of the spool (Fig. 3(a), sky blue).

To reduce the noise of the actuator, the motor, idler, and spool gear are designed with materials with different physical properties (Fig. 3(b)). The gears are also encapsulated and filled with grease (Superlube, Henkel Corp., Susseldorf, Germany). Silicone rubber (Shore 60A) damper is added between the cable-driven actuator and case to isolate actuator vibration to be transferred to the case. The drive noise level is 63 dB at the highest speed, measured with a sound meter from a distance of 60 cm. The experimentally derived specifications of the actuation module are arranged in Table 2.

Table II. Actuation module Specifications

Maximum Tension (nominal)	128 N
Actuation Stroke	270 mm
Speed	550 mm/s
Maximum Noise	63 dB

Note that the tension did not reach targeted value for nominal current, but it could achieve up to 150 N (15 Nm hip torque) using instantaneous maximum current of the actuator.

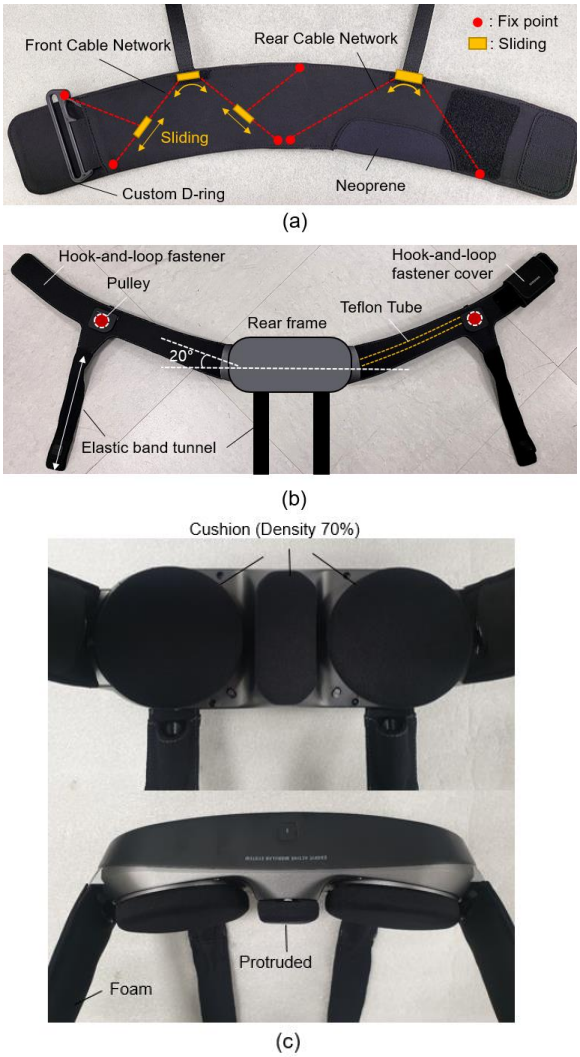

Fig. 4. Design of wearable parts: (a) thigh strap; (b) waist belt; (c) rear frame. Sliding connections are illustrated in yellow blocks and they could slide along cable-networks (yellow arrows).

C. *Rear frame*

The rear frame is designed based on ergonomic considerations (Fig. 1). The human back has a structure where the center is concave and the sides are convex. Additionally, the area around the waist is mostly soft, but there is rigid area around the center where the sacrum, a skeletal structure, is placed. For strong anchoring performance (small deformation with respect to force), the rear frame must come into contact with the sacrum area (Fig. 1). For this reason, the center of the rear frame is designed to protrude by 18 mm with the width of 40 mm so that it could fit into the concave area and contact with the sacrum (Fig. 4(c)). To prevent pain caused by pressure concentration in the sacrum area, the pressure around the back is distributed by placing cushions on the bottom of the actuation module and the protruded area of the rear frame, thereby maximizing the contact area (Fig. 4 (c)).

Main MCU, actuator connectors, and battery pack with four 18650 batteries are placed inside the rear frame. The actuator is powered by 24 V, 10A, and UART communication is conducted with the main MCU.

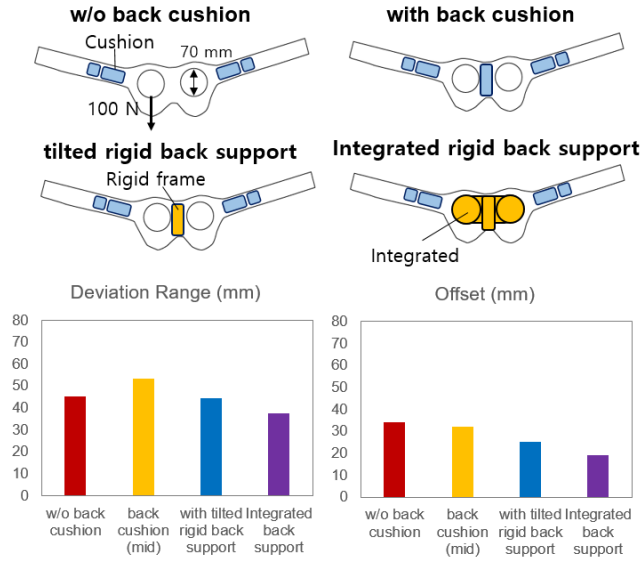

Fig. 5. Comparison of anchoring performance of the waist belt for various structure: deviation is defined as average displacement difference between 0 N and 100 N cable tension condition, and the offset represents displacement before and after the anchoring test experiment repeated 10 times for a single subject.

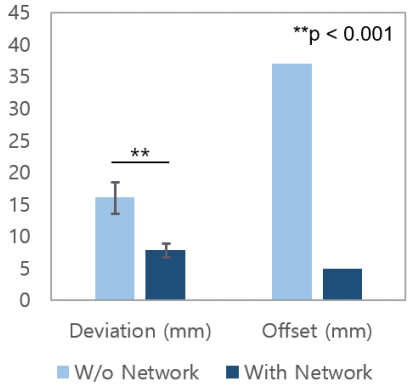

Fig. 6. Comparison of anchoring performance of the thigh strap with and without network structure: deviation is defined as average displacement difference between 0 N and 150 N cable tension condition, and the offset represents displacement before and after the anchoring test experiment repeated 10 times for a single subject.

D. *Waist Belt & Thigh Strap*

The waist belt and thigh straps are designed to increase the anchoring performance by maximizing the contact area according to the cone-shaped thigh and waist shape of a human.

In the case of the waist, the belt is designed in a curved shape with a shorter upper circumference and a longer lower circumference, as the circumference increases from the waist to the pelvis. To create a three-point support for stable anchoring, the angle between the waist belt and the rear frame is set 20° upward, allowing the rear frame to touch the sacrum and the waist belt to touch the iliac crest (Fig.1(a) and Fig. 4(b)). The foam is placed at the iliac crest area to distribute pressure and prevent pain during anchoring (Fig. 4(c)).

The proposed design was selected based on preliminary experiments evaluating the effect of the protrusion around the sacrum and proper stiffness condition for increasing the

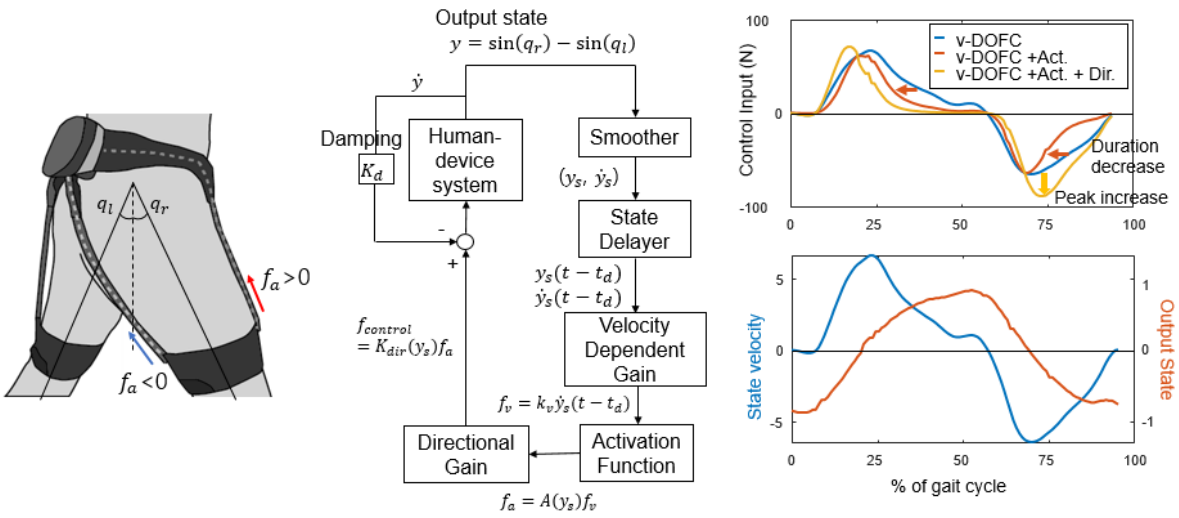

Fig. 7. Controller design: (a) control block diagram, (b) effect of each gain component on control output with respect to output state and velocity. Blue, yellow, and red lines indicate control input calculated from v-DOFC, v-DOFC with activation function, and v-DOFC with activation function and directional weight, respectively.

anchoring performance (Fig. 5). The anchoring performance of split (Fig. 5, circles split) and integrated (Fig. 5, circles connected) actuation module frame design between were also tested using a motion capture system (Optitrack V120, NaturalPoint, Inc., Covallis, OR). The integrated design with rigid protrusion around the sacrum showed the best anchoring results with significantly smaller deviation ($p<0.001$), therefore was implemented in waist belt design. The absolute average deviation of the waist belt during 100 N loading condition is under 40 mm.

A Teflon tube is embedded inside the waist belt for cable routing from the rear frame to the pulley placed near the iliac crest. The cable is then routed downward passing the pulley to the thigh strap to minimize friction. The outer fabric of the waist belt is made of a lightweight fabric (nylon). A paper core with patterned holes is placed inside to prevent deformation. The core material of the pulley area consists of polyvinyl chloride (PVC) sheet.

The thigh strap is designed in a curved shape with a shorter circumference around near the knee and longer circumference around the thigh, to fit the cone-shaped thigh. A deformable material (neoprene) is used for the lower rear part of the strap due to the presence of tendons and nerves near the back of the knee. A cable network is constructed inside the thigh strap to distribute force to the lower and upper sides of the strap when the cable is loaded (Fig. 4(a)). The front network consists of three strands fixed on the strap or custom d-ring at four points, and the rear network consists of a single strand fixed at two points (Fig. 4(a), red dots). Sliding connections are used at connection point between cables, for even distribution of force to each strand despite of the force direction.

The outer fabric, and core material of the waist belt are made of the same material as the waist belt, and PVC material is placed near the area where the cable is fixed (Fig. 4 (a)). The effect of the cable network structure on the anchoring performance was tested prior to the thigh strap design (Fig. 6). The deviation of the thigh strap during 150 N loading was under 10 mm with the cable network structure. Significantly smaller deviation was observed ($p < 0.001$) for the thigh strap with network structure (Fig. 6).

III. Controller Design

A. Overview

Many existing cable-driven devices use sensors such as force sensors or IMU to control the system, as it is difficult to accurately estimate the angle due to slack and compliance of the cable. In our research group, delayed output feedback control (DOFC) is developed and used for a hip assist exoskeleton [3]. DOFC only uses angle information obtained from the motor encoder and effectively reduces metabolic cost for walking gait. DOFC algorithm requires clear hip angle sensing to work well.

In this study, we introduce an algorithm that provides a delayed output based on the velocity state instead of angle information. Since it is known that the magnitude of the assist force suitable for extension and flexion is different [6, 7], we also applied the different magnitude for each direction. The overall control block diagram is as in Fig. 6(a).

B. Velocity dependent DOFC (v-DOFC)

The output state is defined as follows:

$$y = sin(q_{right}) - sin(q_{left}) \quad (1)$$

Where q_{right} and q_{left} are the hip flexion angle of the right and left side, respectively. The output state was low-pass filtered as follows to smooth out the control input.

$$y_s = (1-\alpha)y(t) + \alpha y(t - t_{sample}) \quad (2)$$

Where, $0 < \alpha < 1$, and t_{sample} is the sampling time. The assistance force of the velocity dependent delayed output feedback controller (v-DOFC) input with the time delay of t_d is as follows:

$$f_v = k_v \dot{y}_s(t - t_d) \quad (3).$$

Where, f_v is the velocity dependent assistance force, k_v is the velocity dependent gain.

C. Activation Function

To allow movement without interference when the hip is in fully flexed or extended posture, an activation function $A(y_s)$ with the weight reducing as the magnitude of state y_s increases was implemented. The activation function also serves to alleviate fluctuations due to cable slack. The control input with the activation function applied is as follows:

$$\sigma(y_s) = \frac{1}{1 + e^{-k_a y_s (t - t_d)}} \quad (4),$$

$$A(y_s) = 4\sigma\,(1 - \sigma) \quad (5),$$

$$f_a = A(y_s) k_v \dot{y}_s (t - t_d) \quad (6).$$

The activation function $A(y_s)$ also act as adjusting the time duration of assistance for the same speed. The time duration decreases as k_a increases, as the decrease of $A(y_s)$ with respect to $|y_s|$ becomes steeper.

D. Directional Weight

Previous studies have showed that the optimal assistance level of extension is greater than that of flexion for decreasing metabolic cost of walking [6, 7]. Directional weight function is applied to differentiate the assistance level of flexion and extension. The overall assistance force including directional weight is as follows:

$$K_{dir}(y_s) = e^{k_{dir} y_s (t - t_d)} \quad (7),$$

$$f_{control}(y_s, \dot{y}_s) = K_{dir}(y_s)\mathrm{A}(\mathrm{y_s})\mathrm{k_v}\dot{y}_s(t - t_d) \quad (8).$$

When $k_{dir} < 0$, the extension assistance is relatively greater than the flexion, and when $k_{dir} > 0$, the flexion assistance is relatively greater. The directional weight $K_{dir}(y_s)$ also acts as an adjusting factor for the peak assist timing. In the case where $k_{dir} < 0$, the flexion peak assist timing gets earlier, while the extension peak assist timing is delayed. When $k_{dir} > 0$, the flexion peak assist timing is delayed, while the extension peak assist timing gets earlier.

The effect of each weight function on the control input is shown in Fig. 7(b).

E. Damping

A damping term is added to prevent oscillation that occurs in high control gain condition due to compliance and slack of the cable. The gain is heuristically set to minimum value not to affect the assist timing while preventing oscillation. The control input then becomes,

$$f_{control}(y_s, \dot{y}_s) = K_{dir}(y_s)\mathrm{A}(\mathrm{y_s})\mathrm{k_v}\dot{y}_s(t - t_d) - K_d\dot{y}(t) \quad (9).$$

IV. Experimental Methods

A. Experimental Protocol

The effectiveness of the device was evaluated by comparing the metabolic cost. Three healthy subjects (3 male subjects, age [mean±SD]: 31.6±6.3 yrs) participated in the metabolism experiment.

The experimental protocol was designed to measure the changes in metabolic effort of walking without the device, wearing the proposed device without assistance, and with device assistance. The protocol aims to evaluate the effect of the weight of the device and the effect of assistance.

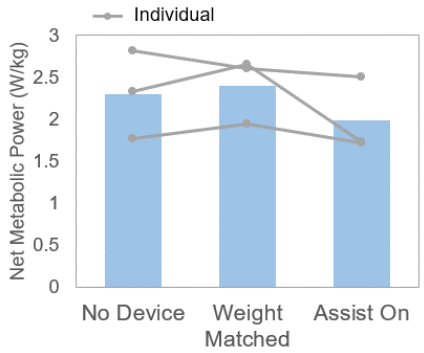

Fig. 8. Comparison of net metabolic cost of walking

The subjects first rested in standing position for 5 min. Then, they walked on the treadmill for 5 min at a speed of 4 km/h in three different conditions: without the device (No Device), with the device but without assistance (Weight-matched), and with the device providing assistance (Assist On). After each condition, the subjects rested for another 5 min. In the conditions with the device but without assistance, the thigh strap was left unworn, and only the waist belt was worn. This was done to include only the effect of the weight of the device, while excluding the effect of the motor inertia and the force provided by the flexible band tunnel. The controller gain was heuristically selected based on pretests and set as follows for each subject.

Table III. Control Parameter Setting

Subject	k_v	k_a	k_{dir}	K_d	t_d(ms)
S1	21	3.8	1.9	5.75	5
S2	21	3.8	1.9	5.75	5
S3	24	3.8	1.9	6.35	5

B. Data Analysis

The metabolic cost was assessed using the Cosmed K5 (Cosmed, Rome, Italy). The metabolic power was calculated by the Brockway equation [11], which is a common standard used to evaluate the rate of metabolic energy consumption. Net metabolic power was calculated by subtracting the average metabolic power of standing phase. The average metabolic power of the last 2 min of each phase when steady state had been reached was used for analyzing the percent reduction.

V. Results

When the subjects are assisted by the device (Assist On), there is an overall reduction of net metabolic power by 13.8%, compared to walking without the device (No Device, Fig. 8). When the proposed device is worn (Weight-matched), the net metabolic power increases by 4.2%, compared to walking without the device (No Device). When the subject is assisted by the device (Assist On), there is a reduction of 17.3%, compared to no assistance (Weight-matched).

The effect of the device differed among subjects. Subject S1 and S3 showed an increase in metabolic power when the device was worn, while subject S2 showed a decrease in metabolic power. This difference in results may be attributed

to the fact that free walking test was conducted prior to walking with the device, which may have led to a decrease in metabolic cost due to familiarization with the treadmill. The disadvantage of the weight of the device was found to be small enough to be overcome by the advantage of assistance provided by the device. The reduction of net metabolic cost with device assistance is 2.8%, 11.0 %, 25.4 % for subject S1, S2, and S3, respectively.

VI. Discussion and Conclusion

We have developed a lightweight, bi-directional cable-driven hip assist device, prioritizing anchoring with ergonomic considerations. The rear frame and waist belt's shape (Fig. 4(b-c)) ensure stable anchoring on three rigid points, minimizing deformation around the skeletal structure (one on the sacrum and two on each side of the iliac crest, Fig. 1). Incorporating cushions around anchoring point mitigated discomfort around the anchoring points during assistance.

The embedded cable network structure (Fig. 4(a)) evenly distributes force on the strap's upper and lower parts, increasing the contact area on the thigh due to curved shape of the strap. This design achieves stable anchoring by compressing both upper and lower thigh portions when cable tension is applied. The sliding connection ensures even force distribution along each cable strand, independent of pulling direction (Fig. 4(a)).

Every component of the proposed device was designed for minimal weight, resulting in a 1.5 kg total weight, including bi-directional actuators. Despite the device's weight, its benefits in assistance outweighed the disadvantages reducing the metabolic cost of walking (Fig. 8). Subject S3 noted that the weight concentration around the rear waist seems to aid in maintaining upright posture while walking.

The flexible band tunnel connecting the waist and thigh straps not only prevents the thigh strap from slipping downward but also acts as a parallel elastic component. The effect of the elasticity has reduced the metabolic power of walking for subject S2 and S3, observed from preliminary tests. This is consistent with the results of several studies [12, 13], which show that passive hip flexion with elastic components can reduce the metabolic power for walking and running. By combining the elastic component with active assistance, a greater assistance force can be applied compared to a system that only includes active assistance. We anticipate that the optimal selection of elastic components will help reduce the required power of the actuator and eventually decrease the overall weight of the system.

Bi-directional actuation with the novel v-DOFC control method allowed hip flexion and extension assistance using motor encoder measurements only. The velocity-dependent controller enabled control independent of accurate sensing of hip angle, as the activation gain primarily responds to the rate of change of state rather than the state itself. The damping term attenuated potential that can occur due to slack. The directional gain term which could differentiate the assistance level of flexion and extension, significantly influenced the performance in reducing the metabolic power. The reduction of metabolic power was higher when greater assistance was provided on extension.

This study has several limitations that must be addressed in future studies. First, while the proposed v-DOFC can compensate for slack, it is still challenging to respond when the slack is large. To address this limitation, a mechanism for automatically adjusting the cable length should be developed. Secondly, the controller parameters were heuristically adjusted to each subject, and further analysis should be conducted to evaluate the effect of each gain parameter on the walking assist performance. Additionally, an optimization algorithm for determining the optimal parameters should be developed. Thirdly, the effectiveness of this device has only been tested for a small number of participants. To generalize the findings to a larger population, additional evaluation should be conducted. Lastly, while the effect of the elastic component was observed for several subjects on decreasing the metabolic cost, the analysis was not conducted in-depth. Further study should be conducted to evaluate the effect of the elastic component and active assistance separately, and investigate the advantage of combined use.

References

[1] H. Shimada, et al., "Effects of a robotic walking exercise on walking performance in community-dwelling elderly adults," *Geriatr. Gerontol Int*, vol. 9, no. 4, pp. 372-381, May 2009.

[2] K. Yasuhara, K. Shimada, T. Koyama, T. Ido, K. Kikuchi, and Y. Endo, "Walking assist device with stride management system," *Honda R&D technical review,* vol. 21, no. 2, pp. 54-62, Aug. 2009.

[3] B. Lim, J. Lee, J. Jang, K. Kim, Y. Park, K. Seo, and Y. Shim, "Delayed output feedback control for gait assistance with a robotic hip exoskeleton," *IEEE Trans* Robot, vol. 35, no. 4, pp. 1055-1062, Aug. 2019.

[4] Y. Lee, et al., "A flexible exoskeleton for hip assistance," 2017 IEEE/RSJ International Conference on Intelligent Robots and Systems (IROS), Vancouver, BC, Canada, 2017, pp. 1058-1063

[5] S. Yu, et al., "Quasi-Direct Drive Actuation for a Lightweight Hip Exoskeleton with High Backdrivability and High Bandwidth," *IEEE/ASME Trans Mechatron*, vol. 25, no. 4, pp. 1794-1802, May 2020.

[6] J. Kim et al., "Reducing the energy cost of walking with low assistance levels through optimized hip flexion assistance form a soft exosuit," *Sci Rep*, vol. 12, no. 11004, pp. 1-13, June 2022.

[7] J. Kim et al., "Reducing the metabolic rate of walking and running with a versatile, portable exosuit," *Science*, vol. 365, no. 6454, pp. 668-672, 2019.

[8] J. Yang, J. Moon, J. Ryu, J. Kim, K. Nam, S. Park, Y. Kim, and G. Lee, "Design of a Quasi-Direct Drive Actuator with Embedded Pulley for a Compact, Lightweight, and High-Bandwidth Exosuit," *Actuators,* vol. 12, no. 1, pp. 21, Dec. 2023.

[9] W. Cao, et al. "Effect of Hip Assistance Modes on Metabolic Cost of Walking With a Soft Exoskeleton," IEEE Tras Autom Sci Eng, vol. 18, no. 2, pp. 426-436, April 2021.

[10] J. Kim, J. Moon, S. Park, and G. Lee, "Characterizing force capability and stiffness of hip exosuits under different anchor points," *Plos One*, vol. 17, no. 8, pp. 1–19, Aug. 4, 2022.

[11] J. M. Brockway, "Derivation of formulae used to calculate energy expenditure in man," *Hum Nutr Clin Nutr*, vol. 41, no. 6, pp. 463-471, Nov. 1987.

[12] J. Yang, J. Park, J. Kim, S. Park, and G. Lee, "Reducing the energy cost of running using a lightweight, low-profile elastic exosuit," *J Neuroeng Rehabil*, vol. 18, no. 129, pp. 1–12, Aug. 2021.

[13] F. A. Panizzolo, C. Bolgiani, L. Di Liddo, E. Annese, and G. Marcolin, "Reducing the energy cost of walking in older adults using a passive hip flexion device," *J Neuroeng Rehabil*, vol. 16, no. 117, pp. 1-9, Oct. 2019.